Formation of Zn-Containing Clusters in an Implanted Si₃N₄/Si Film

A. N. Tereshchenko[a], *, **V. V. Privezentsev**[b], **A. A. Firsov**[b], **V. S. Kulikauskas**[c],
V. V. Zatekin[c], **and M. I. Voronova**[d]

[a] *Osipyan Institute of Solid State Physics, Russian Academy of Sciences, Chernogolovka, Moscow region, 142432 Russia*
[b] *Federal Research Center "Scientific Research Institute for System Analysis," Russian Academy of Sciences, Moscow, 117218 Russia*
[c] *Lomonosov Moscow State University, Skobeltsyn Institute of Nuclear Physics, Moscow, 119991 Russia*
[d] *National University of Science and Technology "MISiS," Moscow, 119049 Russia*
*e-mail: tan@issp.ac.ru

Abstract—The results of the synthesis and study of Zn-containing clusters at the interface of a Si₃N₄/Si film implanted with $^{64}Zn^+$ ions with a dose of 5×10^{16} cm^{-2} and an energy of 40 keV are presented. A Si₃N₄ film is preliminarily deposited onto a silicon substrate using the CVD-method. Then, the implanted samples of 10 × 10 mm are annealed in an oxidizing atmosphere (in air) with a step of 100°C for 1 h at each step in the temperature range from 400 to 800°C. The Rutherford backscattering method is used to study the profiles of zinc during annealing. The structure and composition of the film are studied using scanning electron microscopy in combination with energy-dispersive spectroscopy, as well as photoluminescence. After implantation, individual clusters of metallic zinc with a size of about 100 nm or less are recorded near the surface of the Si₃N₄ film. It is established that, during annealing, Zn clusters grow in the sample and the phase of metallic Zn gradually transforms into phases of its oxide ZnO and then, presumably, silicide Zn₂SiO₄. After annealing at a temperature of 700°C, which is the most optimal for obtaining the ZnO phase, zinc-oxide clusters with a size of about 100 nm are formed in the Si₃N₄ film. A peak appears in the photoluminescence spectrum at a wavelength of 370 nm due to exciton luminescence in zinc oxide. After annealing at 800°C, the ZnO phase degrades and, presumably, the zinc-silicide phase Zn₂SiO₄ is formed.

Keywords: silicon substrate, Si₃N₄ film, zinc implantation, clusters, annealing in an oxidizing environment, zinc oxide

DOI: 10.1134/S1027451023060198

INTRODUCTION

The properties of nanoclusters of metals and their oxides can differ significantly from the properties of the same materials in the macroscopic form. In the nanometer range, these nanoclusters have unique properties, and, therefore, their use in various matrices can be very promising in microelectronic, nanoelectronic, and optoelectronic devices.

In particular, in recent years, there has been a need in microelectronics for light sources in the ultraviolet (UV) region. This stimulated the intensive search for materials with a suitable band gap. The main efforts were concentrated around GaN (E_g = 3.5 eV) and its solid solution with In. However, the binding energy in an exciton for this material is 24.8 meV, so the operating temperature range for using this material is limited [1]. For UV-radiation sources, zinc oxide ZnO is the most suitable material. Interest in this material is due not only to its wide band gap of 3.4 eV, but also to the high binding energy between an electron and a hole in an exciton equal to 60 meV [2], which is much higher than that of GaN. This makes it possible to implement radiation generation in ZnO based on exciton recombination at temperatures above room temperature.

Generally speaking, zinc oxide has been studied for a long time [3] and is widely used in microelectronics, in particular, to create transparent contacts to various optical elements [4]. In addition, since ZnO is a piezoelectric, it is widely used in the creation of delay lines for surface acoustic waves and other acoustic-electronic devices [5]. Due to the sorption effect, zinc oxide has found application in gas sensors and similar chemical sensors for biology and medicine [6–8]. Its application in solar cells of a new generation (Gratzel cells) is known [9]. Recently, ferromagnetism at room temperature was discovered in zinc oxide in the form of nanoparticles [10], which is promising for the creation of devices for spintronics based on it. ZnO nanoparticles placed in various matrices, for example,
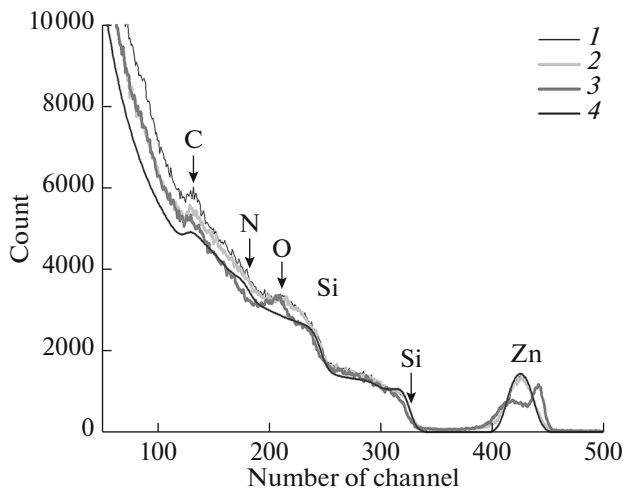
Fig. 1. RBS spectra of the Si_3N_4 film on a silicon substrate: (*1*) after zinc implantation, and after annealing at (*2*) 600 and (*3*) 800°C, and (*4*) calculation.

Si, quartz, SiO_2, and Si_3N_4 films on Si substrate and sapphire can be used in various microelectronic devices. Earlier, Zn and ZnO nanoclusters were created in quartz, SiO_2 films, and silicon, and sapphire implanted with Zn followed by both thermal annealing in an oxidizing environment and photonic annealing in vacuum with additional substrate implantation with oxygen [11−17]. Implantation was chosen because it is one of the cleanest and most flexible technological methods, which allows one to obtain Zn concentrations that are much higher than its limiting equilibrium solubility in various substrates. This contributes to the separation of zinc into precipitates after implantation.

The aim of this research is to study the formation of ZnO clusters in a Si_3N_4 film on a Si substrate after zinc implantation and thermal annealing in an oxidizing environment.

EXPERIMENTAL

Si_3N_4 films with a thickness of 150 nm were obtained by high-temperature chemical vapor deposition (CVD) carried out in an argon flow on standard *n*-type silicon wafers with a diameter of 76 mm and a thickness of 380 μm with the (111) orientation grown by the Czochralski method. The silicon-nitride film was chosen because Si_3N_4, along with silicon oxide SiO_2, is the main dielectric in modern microelectronics. Silicon nitride is used as a mask in the diffusion of various impurities into the silicon substrate and in the oxidation of silicon. Unlike silicon oxide, silicon nitride has a high concentration of electronic traps and is widely used as a medium for storing bound charge in traps; therefore, Si_3N_4 is a promising material for cre-

ating an active layer in the manufacture of resistive memristors (ReRAM devices) [18].

In the experiment, a silicon-nitride film was used as an intermediate layer on silicon to create ZnO clusters in this region. A Si_3N_4 film grown on silicon was implanted with $^{64}Zn^+$ ions at a dose of 5×10^{16} cm^{-2} and energy of 40 keV. During implantation, the ion current did not exceed 0.35 μA/cm^2, so that the wafer temperature was no higher than 40°C. Next, the wafers were cut into samples of 10×10 mm and annealed for 1 h in air at temperatures from 400 to 800°C with a step of 100°C.

To study the changes in the profiles of implanted Zn upon annealing, the Rutherford backscattering (RBS) of $^4He^+$ ions with an energy of 700 keV was carried out using a Van de Graaf accelerator. The energy resolution of the detector—amplifier system was 20 keV and the scattering angle was 160°. The surface of the Si_3N_4 film was examined using a COXEM+ scanning electron microscope (SEM) with a secondary-electron detector in combination with energy-dispersive spectroscopy (EDS) including the display of EDS maps of individual elements and their superposition. To study the change in the phase of zinc during annealing, photoluminescence was used: the spectra were measured at a temperature of 6 K in the wavelength range from 330 to 620 nm. Photoluminescence was excited using a He−Cd laser with a wavelength of 325 nm and a pump power of 0.5 W/cm^2.

RESULTS AND DISCUSSION

Investigation Using Rutherford Backscattering Spectroscopy

Figure 1 shows the experimental RBS spectra of a Si_3N_4 film on a silicon substrate after implantation and annealing with the above parameters, as well as the calculated spectrum (curve *4*) obtained using the SRIM program [19]. This figure clearly shows not only the Zn zone (channels 380−460), but also the "step" corresponding to the silicon substrate (channel 240), the region corresponding to the nitrogen content in the silicon-nitride film (channels 120−185), and, finally, a small peak (near channel 212) corresponding to the oxygen content on the surface of the silicon-nitride film.

Figure 2 shows the experimental RBS spectra of the Zn zone. An analysis of the curves in this figure shows that the Zn profile after implantation is indeed symmetrical and has a normal shape. As is known, the mobility of Zn rather weakly depends on temperature in the range from 400 to 600°C and begins to change to a greater extent at 700°C and higher, when Zn becomes very mobile on account of the fact that it has a mixed diffusion mechanism, for example, vacancy—interstitial mechanism in silicon. In silicon nitride, zinc behaves at high temperatures like other rapidly

diffusing impurities such as noble (Au) or transition metals (Ti, Ni) [20]. During annealing, the profiles of implanted zinc begin to shift first at low temperatures (400−600°C) slightly deeper into the Si_3N_4 film, and then at higher temperatures (700°C and higher) to the surface, which is an unlimited drain for them. The maximum of implanted zinc becomes smaller and broadens, so now its profile is no longer symmetrical.

Investigation Using Scanning Electron Microscopy

Figure 3 shows the SEM image obtained in the secondary-electron-detection mode (topological contrast). In this figure, in the subsurface layer of a silicon-nitride film, individual bright particles (bumps) with a size of 1 μm or less, up to 100 nm, are observed. Figure 4 shows the energy-dispersive spectrum of the same sample after implantation taken from the frame in Fig. 3.

The content of these elements for the same frame is given in Table 1. It follows from Fig. 4 and Table 1 that the subsurface layer of the Si_3N_4 film after implantation contains implanted Zn in an amount of 5.4 at %. The numerical values of the matrix elements of the silicon-nitride film are given in Table 1. The content of other elements is within the error of the method.

Figure 5 shows various SEM images of the sample surface and corresponding EDS maps after annealing at 700°C. From these figures, it becomes clear that the observed nanoparticles consist of zinc oxide, since the maps of silicon (Fig. 5c) and nitrogen (Fig. 5d) contain dark spots proving the absence of these elements in the SEM image (Fig. 5a). Both on the zinc map (Fig. 5e) and on the oxygen map (Fig. 5f), these dark spots correspond to light spots, which confirms the presence of both zinc and oxygen. The light haze in Fig. 5b corresponds to a thin film of hydrocarbons on the silicon-nitride surface. From the above, it becomes clear that the bright particles (bumps) on the surface of the sample after annealing at 700°C (Fig. 5a) are zinc oxide ZnO.

Figure 6 shows the energy-dispersive spectrum of the sample after annealing at 700°C. The element concentrations in the Si_3N_4 layer after annealing at 700°C are given in Table 2. The content of other elements is within the error of the method. It follows from the analysis of Table 2 that a significant amount of oxygen (8.15 at %) appeared in the annealed sample due to the diffusion of oxygen molecules from the surrounding atmosphere (air) during annealing. The content of implanted zinc decreased somewhat both due to its redistribution after annealing and due to reverse diffusion into the surrounding atmosphere (as noted above, the implanted zinc shifts to the sample surface during high-temperature annealing). A certain amount of carbon appeared in the energy-dispersive spectrum probably because of annealing in air.
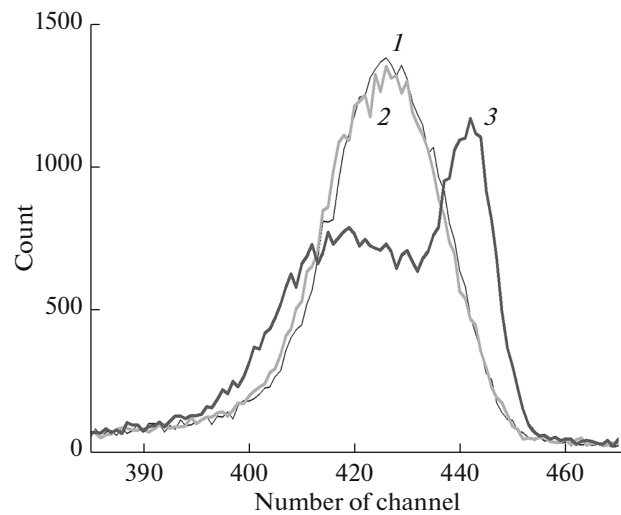

Fig. 2. Experimental RBS spectra in the Zn zone (*1*) after implantation, and after annealing at (*2*) 600°C and (*3*) 800°C
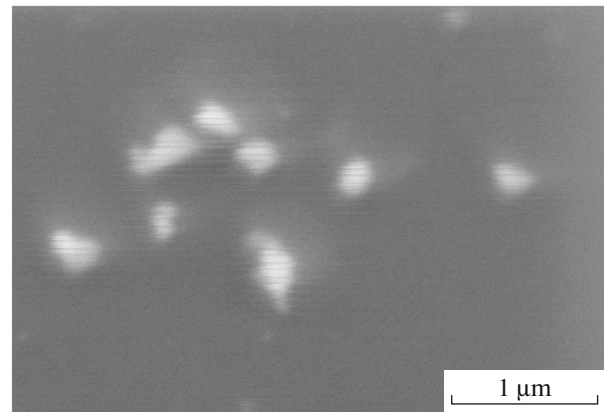

Fig. 3. Overview SEM image of the sample surface after Zn implantation obtained in the secondary-electron-detection mode.
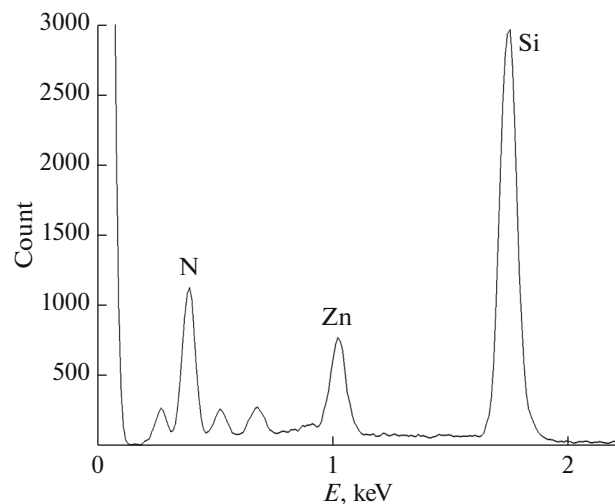

Fig. 4. Energy-dispersive spectrum of a silicon-nitride film after implantation over the frame in Fig. 3.

Table 1. Content of elements in the Si_3N_4 film after implantation

Element	Type of line	Concentration, at %
Si	K series	49.95
N	K series	43.65
Zn	L series	5.40
Total		100.00

On the basis of the above for the annealed sample, we assume that the bright spots (bumps) in Fig. 5 are Zn-containing nanoparticles presumably of ZnO composition and possibly with a small amount of the Zn_2SiO_4 phase.

Photoluminescence

Figure 7 shows the photoluminescence spectra of the samples implanted and annealed in air in the temperature range from 400 to 800°C with a step of 100°C. It follows from the figure that after implantation of the Si_3N_4 film with $^{64}Zn^+$ ions, the photoluminescence signal is almost absent. After first thermal annealing at 400°C, the signal slightly increased; now the spectrum is a broad band with a maximum at about 420 nm, which is probably related to the formation of radiation-induced point defects and their clusters in the Si_3N_4 film [21]. Annealing at 500°C and 600°C leads to an increase in the intensity of the observed broad photoluminescence band without a change in the structure of the spectrum, and the spectral distribution of the luminescence intensity is preserved. After
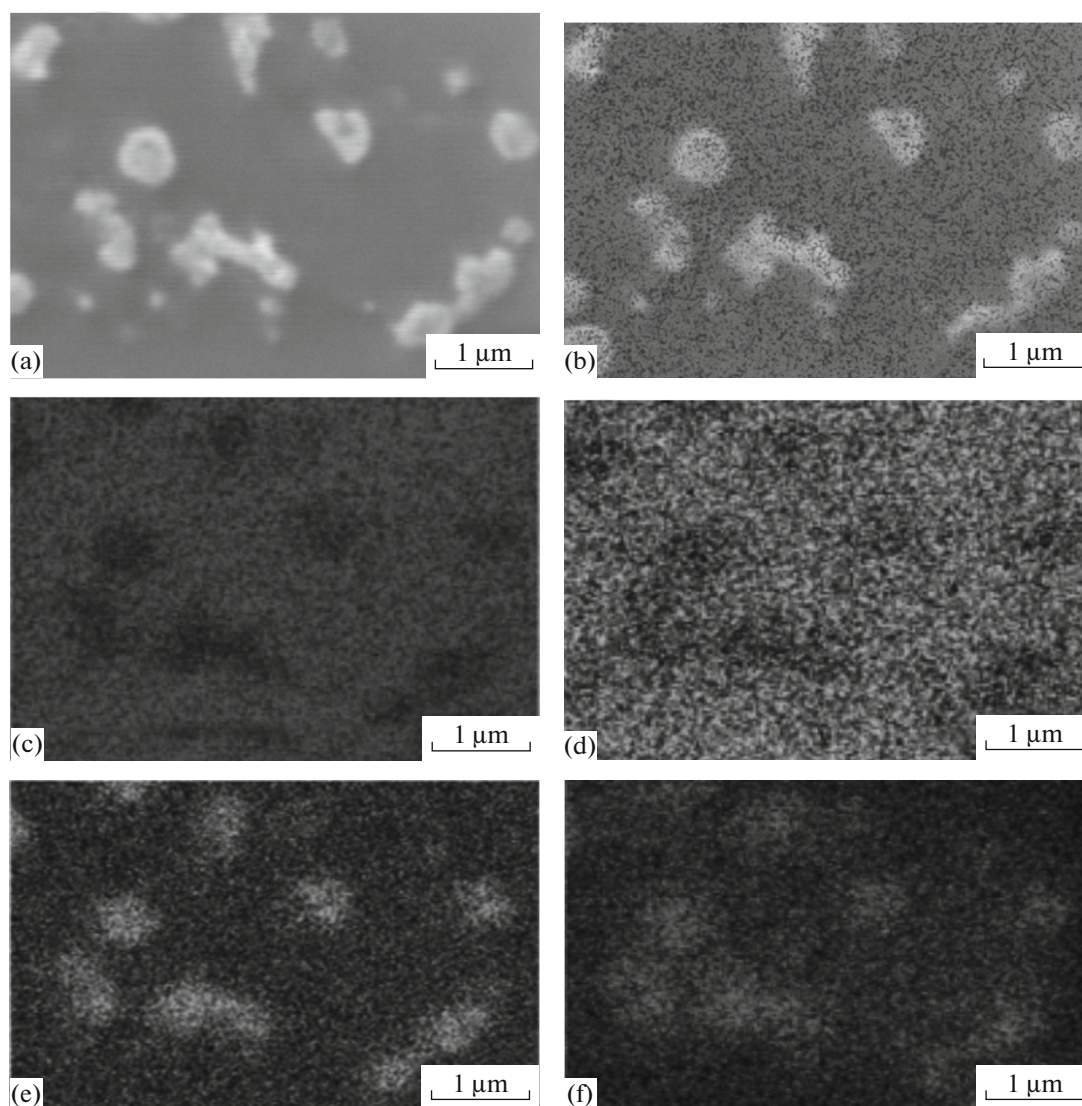

Fig. 5. (a) SEM image of a silicon-nitride film obtained in the secondary-electron-detection mode and corresponding EDS maps of the surface after annealing at 700°C: (b) multilayered for C, O, N, Zn, and Si; (c) for $SiK_{\alpha1}$, (d) for $NK_{\alpha1}$, (e) for $ZnL_{\alpha1,2}$, and (f) for $OK_{\alpha1}$.
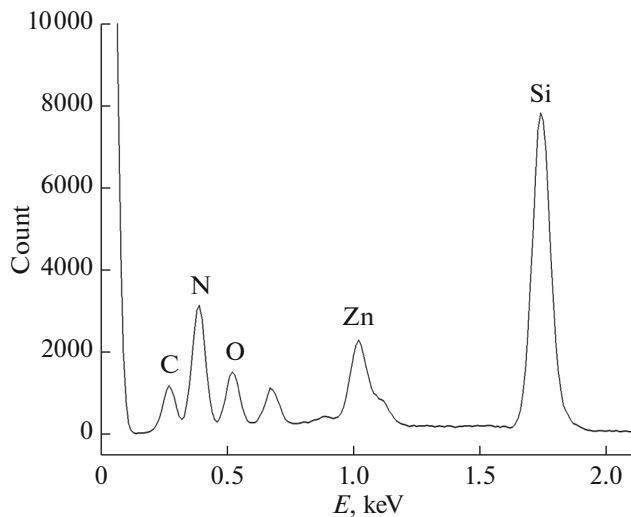
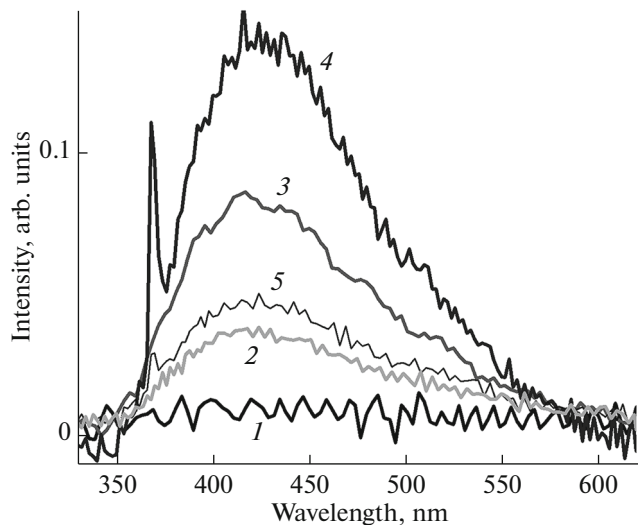**Fig. 6.** Energy-dispersive spectrum of a silicon-nitride film after annealing at 700°C over the frame in Fig. 5.

Fig. 7. Photoluminescence spectra of a Si_3N_4/Si film (*1*) implanted with Zn and then annealed at (*2*) 400, (*3*) 600°C, (*4*) 700°C, and (*5*) 800°C, correspondingly.

Table 2. Content of elements in the Si_3N_4 film after annealing at 700°C

Element	Line	Concentration, at %
Si	*K* series	42.49
N	*K* series	41.37
Zn	*L* series	4.38
O	*K* series	8.15
C	*K* series	2.3
Total		100.00

annealing at 700°C, the photoluminescence intensity continues to increase, and a narrow line appears in the spectrum at a wavelength of 370 nm, which is related to exciton recombination in the ZnO phase. In other words, after annealing in air at a temperature of 700°C for 1 h, a stable ZnO phase appears in the Si_3N_4 film [22]. After annealing at 800°C, strong quenching of the intensity of the broad photoluminescence band is observed; this may be related to the annealing of radiation-induced point defects and their clusters in the Si_3N_4 film. There is also strong quenching of the peak intensity at a wavelength of 370 nm, which indicates degradation of the ZnO phase in the silicon-nitride film, for example, because of the transformation of the ZnO phase into the Zn_2SiO_4 phase. Obviously, during high-temperature stepwise annealing, Zn atoms move from their position after implantation (maximum at a depth of $R_p = 20$ nm) mainly to the surface, which is an unlimited sink for them.

CONCLUSIONS

After the implantation of a Si_3N_4 film with $^{64}Zn^+$ ions with an energy of 40 keV and a dose of 5×10^{16} cm^{-2}, at a depth of about $R_p = 20$ nm and on the surface of silicon nitride, metallic Zn clusters with an average size of 100 nm or less were synthesized. During successive isochronous stepwise annealings in an oxidizing atmosphere (in air) for 1 h at each step of 100°C in the temperature range from 400 to 800°C, the transformation of the metallic Zn phase into the oxide (ZnO) and silicide (Zn_2SiO_4) phases occurred. After annealing at 700°C, the Zn-containing clusters consisted predominantly of the ZnO phase with an average size of about 100 nm. After annealing at 800°C and above, the clusters consist predominantly of the Zn_2SiO_4 phase.

FUNDING

CONFLICT OF INTEREST

The authors declare that they have no conflicts of interest.

REFERENCES

1. N. H. Nickel and E. Terukov, *Zinc Oxide—A Material For Micro- and Optoelectronic Applications* (Springer, Dordrecht, 2005).
2. Ü. Özgur, Ya. I. Alivov, C. Liu, et al., J. Appl. Phys. **98**, 041301 (2005).

3. I. P. Kuz'mina and V. A. Nikitenko, *Zinc Oxide: Obtaining and Properties* (Nauka, Moscow, 1984) [in Russian].

4. C. W. Litton, T. C. Collins, and D. S. Reynolds, *Zinc Oxide Materials for Electronic and Optoelectronic Device Application* (Wiley, Chichester, 2011).

5. Y. X. Liu, Y. C. Liu, D. Shen, et al., J. Cryst. Growth **240**, 152 (2002).

6. Y. Urfa, V. Çorumlu, and A. Altindal, Mater. Chem. Phys. **264**, 124473 (2021).

7. S. Sirelkhatim, A. Mahmud, N. H. M. Seeni, et al., Nano-Micro Lett. **7**, 219 (2015).

8. S. Inbasekaran, R. Senthil, G. Ramamurthy, and T. P. Sastry, Int. J. Innovation Res. Sci. Eng. Technol. **3**, 8601 (2014).

9. G. P. Smestad and M. Gratzel, J. Chem. Educ. **75**, 752 (1998).

10. B. B. Straumal, A. A. Mazilkin, S. G. Protasova, et al., Phys. Rev. B **79**, 205206 (2009).

11. H. Amekura, M. Ohnuma, N. Kishimoto, Ch. Buchal, and S. Mantl, J. Appl. Phys. **104**, 114309 (2008).

12. H. Amekura, Y. Takeda, and N. Kishimoto, Mater. Lett. **222**, 96 (2011).

13. J. Yang, X. Liu, L. Yang, et al., J. Alloys Compd. **485**, 743 (2009).

14. Y. Shen, Z. Li, X. Zhang, et al., Opt. Mater. **32**, 961 (2010).

15. D. Zatsepin, A. Zatsepin, D. W. Boukhvalov, et al., J. Non-Cryst. Solids **432**, 183 (2016).

16. C. Y. Jiang, X. W. Sun, G. Q. Lo, et al., Appl. Phys. Lett. **90**, 263501 (2007).

17. V. V. Privezentsev, A. V. Makunin, A. A. Batrakov, et al., Semiconductors **52**, 645 (2018).

18. S. Kim, H. Kim, S. Jung, et al., J. Alloys. Compd. **663**, 419 (2016).

19. J. F. Ziegler and J. P. Biersack, SRIM. http://www.srim.org.

20. J. Pelleg, in *Mechanical Properties of Materials*, Ed. by J. R. Barber, Solid Mechanics and Its Applications, Vol. 190 (Springer, New York, 2013), p. 85.

21. B. Lin, Z. Fu, and Y. Jia, Appl. Phys. Lett. **79**, 943 (2001).

22. P. A. Rodnyi and I. V. Khodyuk, Opt. Spectrosc. **111**, 776 (2011).

Translated by S. Rostovtseva